3-1-1998

A statistical study of the magnetic signatures of FTEs near the dayside magnetopause

Jeff Sanny
Loyola Marymount University, jeff.sanny@lmu.edu

C. Beck
Loyola Marymount University

D. G. Sibeck
Johns Hopkins University

JOURNAL OF GEOPHYSICAL RESEARCH, VOL. 103, NO. A3, PAGES 4683–4692, MARCH 1, 1998

A statistical study of the magnetic signatures of FTEs near the dayside magnetopause

J. Sanny and C. Beck

Physics Department, Loyola Marymount University, Los Angeles, California

D. G. Sibeck

Applied Physics Laboratory, The Johns Hopkins University, Laurel, Maryland

Abstract. During magnetopause crossings, the AMPTE CCE satellite frequently observed flux transfer events (FTEs) characterized by fluctuations in the magnetic field strength (B) and bipolar signatures in the field component (B_N) normal to the nominal magnetopause. In this study, we survey 110 events observed from October to December 1984 and during January 1986. Nearly all events exhibited increases in B, and although the majority of events exhibited a symmetric bipolar signature in B_N, a significant number (31 of 110) had asymmetric bipolar signatures in which the trailing pulse was dominant. Most of the asymmetric events were observed near the magnetic equator. This is consistent with an explanation in which FTEs form via merging along a single subsolar X line with strongly asymmetric signatures but that these signatures evolve into the familiar symmetric bipolar form with distance from the merging line.

1. Introduction

Transient (~1-min) variations in magnetic field, plasma, and energetic particle parameters are common in the vicinity of the dayside magnetopause. The magnetic field frequently exhibits a bipolar fluctuation in its component normal to the nominal magnetopause accompanied by an increase in the total magnetic field strength. *Russell and Elphic* [1978] named such transients flux transfer events, or FTEs. They interpreted the events as evidence for patchy (localized), sporadic merging between magnetosheath and magnetosphere resulting in the formation of spatially limited flux tubes (or ropes) of reconnected magnetic field lines. The passage of such flux tubes must disturb the surrounding media and produce observable magnetic and plasma perturbations. Using HEOS 2 plasma and magnetic field data, *Haerendel et al.* [1978] independently recognized this phenomenon and deduced its origin as sporadic merging.

By contrast, *Sibeck et al.* [1989] reported that events marked by bipolar magnetic field signatures normal to the nominal magnetopause and magnetic field strength increases can be associated with large-amplitude pressure pulses generated within the foreshock, a result obviating the need to invoke magnetic merging at the magnetopause. Recent simulations by *Lin et al.* [1996a, b] confirm the possibility that even rotational discontinuities can launch pressure/flow variations that disturb the magnetopause, but the origin of transient events observed in the vicinity of the magnetopause continues to be hotly debated [e.g., *Song et al.*, 1994, 1996; *Sibeck and Newell*, 1995, 1996].

Occurrence patterns versus interplanetary magnetic field (IMF) orientation may be helpful in distinguishing between the two proposed causes. If the events are produced by magnetic merging, they should be more common on the equatorial magnetopause during periods of southward IMF orientation, when magnetopause current strengths and instability growth rates increase. By contrast, pressure pulses and the magnetospheric events which they produce should be equally common during intervals of northward and southward IMF orientation. Several statistical surveys support the notion that the majority of events observed in the immediate vicinity of the dayside magnetopause are produced by bursty merging [*Rijnbeek et al.*, 1984; *Berchem and Russell*, 1984; *Southwood et al.*, 1986; *Kuo et al.*, 1995] but indicate that most events observed deeper within the magnetosphere are produced by pressure pulses [*Kawano et al.*, 1992; *Borodkova et al.*, 1995; *Sanny et al.*, 1996].

Numerical simulations describing in detail the signatures expected for FTEs produced by patchy merging have not yet been published. Consequently, this mechanism cannot be tested through detailed comparison with observations. On the other hand, numerous researchers have presented the results of numerical simulations for FTEs produced by bursty merging along extended single and multiple X lines [*Lee and Fu*, 1985; *Ding et al.*, 1986; *Scholer*, 1988; *Shi et al.*, 1988; *Southwood et al.*, 1988; *Ku and Sibeck*, 1997]. Their efforts are justified by observations which indicate a great spatial extent for FTEs [e.g., *Lockwood et al.*, 1990] and the fact that FTEs on the magnetopause can often be described rather well in terms of two-dimensional models [*Farrugia et al.*, 1987; *Walthour et al.*, 1993, 1994]. Since simulations for magnetic merging along extended single and multiple X lines predict strikingly different signatures (e.g., *Ding et al.* [1991]), it should be possible to determine which of these two models is more consistent with the observations and therefore more appropriate to conditions at the dayside magnetopause. Note that there is a transition from multiple to single X line reconnection as system lengths, reconnection rates, or resistivity decrease; all three parameters are difficult to specify [*Lee and Fu*, 1986].

We begin with a review of two-dimensional magnetohydrodynamic (MHD) models and simulations of FTEs. To ensure that

Paper number 97JA03246.
0148-0227/98/97JA-03246$09.00

our database is dominated by FTEs and not pressure-pulse–driven events, we identify FTEs in Charge Composition Explorer (CCE) observations made in the immediate vicinity of the magnetopause, i.e., in the magnetosheath or in the magnetosphere within 30 min of a magnetopause crossing. For comparison with model predictions, we survey the observations as a function of latitude and longitude across the face of the dayside magnetopause.

2. Magnetic Signatures of FTEs Determined From Two-Dimensional MHD Simulations

Various two-dimensional MHD models and simulations have been presented to explain the features of FTEs using the assumption that they are produced by magnetic merging. Some of these simulations are based on the premise that merging takes place along a single X line (e.g., *Scholer* [1988]; *Southwood et al.* [1988]; *Ku and Sibeck*, [1997]), whereas others invoke multiple X line merging (e.g., *Lee and Fu* [1985]; *Ding et al.* [1986]; *Shi et al.* [1988]). *Ding et al.* [1991] compare these two types of simulations.

2.1. Magnetic Merging at a Single X Line

Two-dimensional MHD simulations invoking the onset of merging at a single X line produce monopolar magnetic field signatures (B_N) normal to the nominal magnetopause in the vicinity of the X line and strongly asymmetric bipolar signatures away from the X line [*Ding et al.*, 1991; *Ku and Sibeck*, 1997]. Spacecraft entering the events observe magnetic field strength decreases, whereas those that remain outside observe increases. The top panel in Figure 1 presents the magnetic field pattern surrounding an event produced by merging along a single subsolar X line [*Ku and Sibeck*, 1997]. The computational domain is a rectangular box with a dimensionless width of 48 in the x direction, which is normal to the nominal magnetopause and directed into the magnetosheath, and a width of 175 in the z direction, or northward parallel to the magnetopause. A spacecraft at the leading edge of the event (around $z = 60$) observes a small outward B_x. However, when the spacecraft is at the trailing edge (z = 30–40), it observes a large inward B_x. This combination results in an asymmetric bipolar signature in the magnetic field component normal to the magnetopause. Rather similar signatures are predicted along the axis of symmetry for truncated (i.e., noninfinite) merging line segments according to the work of *Ma et al.* [1994].

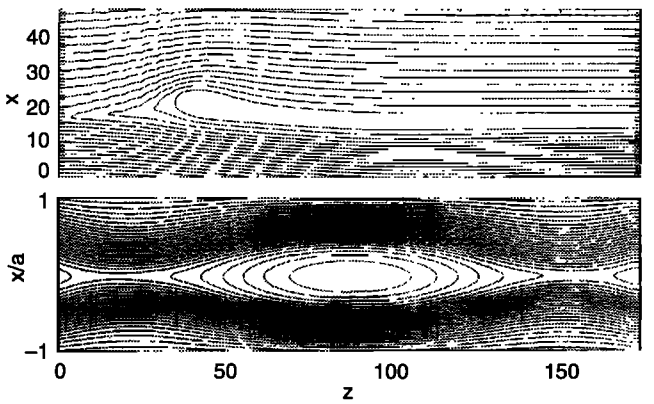

Figure 1. (top) Two-dimensional magnetohydrodynamic (MHD) simulation of the magnetic field pattern surrounding an FTE produced by merging at a single X line. (bottom) Two-dimensional MHD simulation of the magnetic field pattern surrounding an FTE produced by merging at multiple X lines.

The amplitude of the FTE signature depends on the ratio of the magnetospheric (B_m) to magnetosheath (B_s) magnetic field strengths. The greater magnetic field strengths within the magnetosphere imply correspondingly greater magnetic curvature forces there. As a result, the transient event lies primarily outside the magnetopause and does not distort magnetospheric magnetic field lines as significantly as such an event in the magnetosheath. As B_m/B_s increases, the amplitude of the variation in B_N decreases for both magnetosheath and magnetospheric FTEs [*Ding et al.*, 1991]. Furthermore, if B_m/B_s exceeds a certain value (1.5 according to *Scholer* [1988]; 1.7 according to *Ding et al.* [1991]), then the magnetic signatures of magnetospheric FTEs fail to exceed detectability thresholds. In particular, the models predict nearly insignificant magnetospheric B_N signatures for typical ratios of the magnetospheric to magnetosheath magnetic field strengths.

Ku and Sibeck [1997] compare the magnetic perturbations associated with an FTE and the ratios of the leading to the trailing pulse amplitudes in B_N at two different latitudes. At the higher latitude (i.e., at a greater distance from the X line), they find that the perturbation amplitudes as well as the pulse ratio increase. The increase in this ratio indicates that the bipolar B_N signatures of FTEs become more symmetric with distance away from the reconnection line.

2.2. Magnetic Merging at Multiple X Lines

Ding et al. [1991] discuss the FTE signatures that are generated by merging at multiple X lines in terms of magnetic islands. The bottom panel of Figure 1 presents the magnetic field pattern produced by bursty merging at a pair of X lines [*Lee and Fu*, 1986]. As in the single X line models, the ratio B_m/B_s plays a critical role in whether a magnetic signature exceeds detectability criteria. However, the conditions for observing FTE signatures are more favorable than in the case of merging at a single X line. It is predicted that signatures can be detected in both the magnetosheath and the magnetosphere provided $B_m/B_s \leq 2.6$ (as compared to 1.5 or 1.7 for the single X line models). Another significant difference is that MHD simulations based on multiple X line merging with equal merging rates at each line produce magnetic field contours that are symmetric at the leading and trailing edges of a transient event (for example, see *Ding et al.* [1991, Figure 2]). Thus an event produced by multiple X line merging can exhibit a symmetric bipolar signature in B_N, whereas events produced at a single X line never exhibit perfectly symmetric B_N signatures. This is a strong feature in favor of the multiple X line model since past surveys of FTEs near the magnetopause [*Berchem and Russell*, 1984; *Rijnbeek et al.*, 1984] have found their bipolar B_N signatures to be predominantly symmetric. Hence there are clear differences between a model based on merging at a single X line and one based on merging at multiple lines. These models can be easily distinguished by observations near the formation region and with distance away from that region. In a later section, we will report our observations and discuss their consistency with the predictions of the two models.

3. Data Sets

FTEs in the vicinity of the dayside magnetopause were identified by using high time resolution magnetic field data from the AMPTE CCE satellite. The satellite was launched in August 1984 into a near-equatorial orbit with an apogee of 8.8 R_E and an orbital period of 15.7 hours. To determine when the CCE spacecraft made crossings into the magnetosheath, we used data from its charge-energy-mass spectrometer [*Gloeckler et al.*, 1985]. This spectrometer measured the masses and charge-state compositions as well as the energy spectra and pitch-angle distributions of all major ions

from H through Fe with energies from 0.3 to 300 keV/charge at a time resolution of less than 1 min. We used orbital plots of the particle flux of 2-keV H^+ ions with a 6-min time resolution, accessible through the World Wide Web at http://hurlbut.jhuapl:80/AMPTE/summary_images. Periods when the spacecraft crossed into the lower-latitude boundary layer and/or magnetosheath can easily be identified by sharp increases in the particle flux at this energy. We then examined hour-long plots of CCE magnetometer measurements [*Potemra et al.*, 1985] in GSE coordinates at 6.2-s resolution for FTE signatures. When candidate events were found, we performed a minimum variance routine on the magnetopause crossings [*Sonnerup and Cahill*, 1967] and then plotted the observations in boundary normal coordinates.

As stated earlier, we required our events to be observed in the vicinity of the magnetopause to ensure that they were the result of magnetic merging. This requirement was implemented by considering all magnetosheath events but only those magnetospheric events that were within 30 min of a magnetopause crossing. Event signatures ranged from symmetric bipolar to highly asymmetric in the field component normal to the nominal magnetopause, generally accompanied by fluctuations in the other two orthogonal components and centered on fluctuations in the magnetic field strength. Finally, we considered only events whose duration exceeded 1 min and whose peak-to-peak amplitude in B_N was greater than or equal to 5 nT. This is half the cutoff value of 10 nT used by *Rijnbeek et al.* [1984]. All of our smaller-amplitude events were observed in the magnetosphere. On the basis of the signal-to-noise ratio in the data obtained in that region, we felt that the magnetic fluctuations of these smaller-amplitude events were clear FTE signatures that could be retained as part of our data set. The smallest event amplitude in the magnetosheath, with its higher noise level, was 16 nT, which is above Rijnbeek's cutoff value.

4. Statistical Survey

Our data set consists of 110 events observed on 8 separate days, as listed in Table 1. These events were observed from October to December 1984 and during January 1986. Of the events, 84 occurred in the magnetosphere and 26 in the magnetosheath (denoted as regions "M" and "S," respectively, in Table 1). Clearly, this does not imply that FTEs are more commonplace in the magnetosphere than in the magnetosheath. The dominance of magnetospheric events in our data set results from two factors: (1) the relatively low apogee of the CCE and (2) the fact that magnetosheath noise levels generally exceed those in the magnetosphere. Many smaller-amplitude events in the magnetosheath may have been masked by this noise, whereas similar events in the magnetosphere were not.

It is interesting to compare the events of this study with those used in the statistical survey made by *Sanny et al.* [1996]. Both data sets are based on CCE magnetometer readings. However, the events in this work are observed in the immediate vicinity of the magnetopause and are assumed to be FTEs produced by sporadic merging. Those in the work of *Sanny et al.* [1996] are detected in the outer dayside magnetosphere away from the magnetopause and are explained as ripples on the magnetopause surface. The selection criteria for amplitude (4 nT) and duration (1–8 min) in the *Sanny et al.* [1996] work are similar to this study; however, *Sanny et al.* [1996] consider only events with a symmetric B_N fluctuation, while asymmetric signatures are an important part of our survey. There are several fundamental differences between the two data sets. First, the 59 events of *Sanny et al.* [1996] were observed on 25 separate days, indicating that although event recurrence did take place, there were also many isolated events, indicative of the decay of event amplitude with distance from the magnetopause and consequent filtering out of the smaller-amplitude events. In this study, 110 events were detected on 8 separate days, indicating a far greater rate of recurrence, as expected from sporadic merging. For example, the seven events observed between 0100 and 0200 UT, day 280, had an average recurrence time of 7.5 min. Later that day, five events observed between 2300 and 2400 UT were found to have the same recurrence time. Only one of the eight days used in our study appears in the data set of *Sanny et al.* [1996]. This is day 281, in which we observed four events, the last of which is at 1349 UT. A single event at 1439 UT of that day is presented in that paper. Finally, IMF orientation has little or no influence on the events of *Sanny et al.* [1996], whereas nearly all of our events occur for southward IMF.

4.1. Location

Figure 2 shows a plot of event position in the GSM y–z plane. All events surveyed occurred north of the magnetic equator. For this location we expect to observe outward/inward (+/–) B_N perturbations (denoted as the "standard" type event by *Rijnbeek et al.* [1984]). This was indeed found to be the case for 103 out of the 110 events in our data set. In Figure 2, events are denoted by either an asterisk or circle, depending on whether their fluctuations in B_N are asymmetric or symmetric (this will be further discussed in section 4.4).

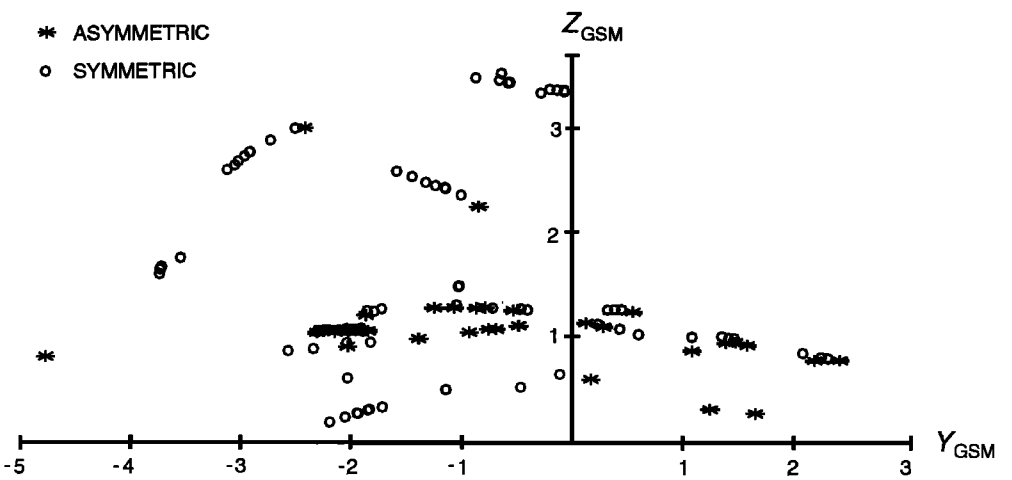

Figure 2. Positions of studied events in the GSM y–z plane.

Table 1. List of events

Day	Event Time, UT	Crossing Time, UT	Event Position in R_E (GSM)	Crossing Position in R_E (GSM)	Region	A, nT	τ, min	Polarity of B_N	α/B	B_m/B_s	θ, deg
				1984							
280	0102	0131	6.62,–2.19,0.268	7.16,–1.81,0.625	M	13	7	+/–	1	6.4	120
	0117	0131	6.90,–2.05,0.311	7.16,–1.81,0.625	M	21	9	+/–	1	6.4	120
	0124	0131	7.07,–1.94,0.343	7.16,–1.81,0.625	M	10	4	+/–	1	6.4	120
	0127	0131	7.07,–1.94,0.346	7.16,–1.81,0.625	M	14	4	+/–	1	6.4	120
	0134	0131	7.24,–1.84,0.368	7.16,–1.81,0.625	M	8	3	+/–	1	6.4	120
	0136	0131	7.24,–1.84,0.374	7.16,–1.81,0.625	M	6	3	+/–	1	6.4	120
	0147	0149	7.39,–1.72,0.400	7.46,–1.78,–0.022	M	9	2	+/–	1	4.8	110
	0332	0347	8.63,–0.457,0.576	8.58,–0.046,0.448	M	11	4	–/+	1	2.1	65
	1819	1805	8.08,–1.14,0.553	7.92,–1.33,0.458	S	156	2	+/–	1	1.6	140
	1821	1805	8.08,–1.14,0.551	7.92,–1.33,0.458	S	31	2	+/–	1	1.6	140
	2300	2322	8.03,2.06,0.848	7.81,2.29,0.803	S	24	5	+/–	1	1.9	175
	2310	2322	7.30,2.18,0.808	7.81,2.29,0.803	M	25	5	+/–	1/5	1.9	175
	2317	2322	7.87,2.23,0.806	7.81,2.29,0.803	M	14	1	–/+	1	1.9	175
	2321	2322	7.81,2.29,0.804	7.81,2.29,0.803	M	14	1	+/–	1	1.9	175
	2330	2322	7.69,2.39,0.799	7.81,2.29,0.803	S	80	1	+/–	1/2	1.9	175
281	1116	1138	8.63,–0.116,0.685	8.63,–0.119,0.684	M	11	4	+/–	1	1.5	175
	1141	1138	8.72,0.175,0.612	8.63,–0.119,0.684	M	13	3	+/–	1/4	1.5	175
	1322	1327	8.63,1.32,0.353	8.61,1.37,0.346	M	44	3	+/–	2/5	3.9	120
	1349	1327	8.46,1.64,0.302	8.61,1.37,0.346	M	8	8	+/–	1/4	3.9	120
292	1657	1647	8.15,1.07,1.00	8.24,0.962,1.01	M	23	5	+/–	1	3.7	170
	1721	1715	7.89,1.34,0.989	7.95,1.29,0.991	M	39	4	+/–	1	1.4	110
	1724	1715	7.85,1.40,0.982	7.95,1.29,0.991	M	9	2	+/–	1/2	1.4	110
	1727	1715	7.85,1.40,0.986	7.95,1.29,0.991	M	11	3	+/–	1	1.4	110
	1731	1715	7.77,1.44,0.984	7.95,1.29,0.991	M	15	1	+/–	1	1.4	110
	1733	1715	7.71,1.50,0.977	7.95,1.29,0.991	M	12	2	+/–	1/3	1.4	110
	1740	1715	7.65,1.56,0.967	7.95,1.29,0.991	M	31	4	+/–	2/3	1.4	110
293	0431	0454	8.19,–1.86,1.23	8.38,–1.55,1.26	M	13	4	+/–	1/2	4.8	115
	0435	0454	8.24,–1.80,1.23	8.38,–1.55,1.26	M	9	3	+/–	1	4.8	115
	0437	0454	8.19,–1.85,1.24	8.38,–1.55,1.26	M	20	4	+/–	1	4.8	115
	0442	0454	8.28,–1.74,1.25	8.38,–1.55,1.26	M	36	8	+/–	1	4.8	115
	0521	0539	8.53,–1.25,1.29	8.58,–1.11,1.30	M	45	2	+/–	1/3	2.2	130
	0534	0539	8.60,–1.05,1.28	8.58,–1.11,1.30	S	65	1	+/–	1	2.2	130
	0548	0555	8.65,–0.857,1.28	8.66,–0.796,1.28	M	15	1	+/–	2/3	1.4	145
	0553	0555	8.66,–0.798,1.28	8.66,–0.796,1.28	M	15	2	+/–	2/5	1.5	145
	0601	0555	8.68,–0.727,1.27	8.66,–0.796,1.28	S	44	2	+/-	1	1.5	145
	0603	0555	8.68,–1.03,1.44	8.66,–0.796,1.28	S	18	2	+/-	1	1.5	145
	0606	0555	8.68,–1.03,1.45	8.66,–0.796,1.28	S	19	2	+/-	1	1.5	145
	0616	0628	8.70,–0.535,1.26	8.70,–0.496,1.24	S	65	2	-/+	2/7	1.6	70

Table 1. (continued)

Day	Event Time, UT	Crossing Time, UT	Event Position in R_E (GSM)	Crossing Position in R_E (GSM)	Region	A, nT	τ, min	Polarity of B_N	α/B	B_m/B_s	θ, deg
				1984							
	0622	0628	8.70,–0.471,1.25	8.70,–0.496,1.24	S	30	5	+/–	1	1.6	70
	0624	0628	8.71–0.410,1.24	8.70,–0.496,1.24	S	19	2	–/+	1	1.6	70
	0703	0717	8.67,0.104,1.15	8.67,0.228,1.12	S	70	2	+/–	1/2	1.8	145
	0713	0717	8.64,0.225,1.12	8.67,0.228,1.12	M	31	2	+/–	1	1.8	145
	0715	0717	8.64,0.227,1.12	8.67,0.228,1.12	M	13	2	+/–	1/3	1.8	145
	0728	0717	8.58,0.415,1.08	8.67,0.228,1.12	S	49	1	–/+	1	1.8	145
	0747	0800	8.51,0.588,1.02	8.42,0.784,0.966	S	86	3	–/+	1	1.6	85
	0826	0800	8.23,1.08,0.856	8.42,0.784,0.966	S	50	3	+/–	1/2	1.4	85
	1920	1921	7.65,–2.57,0.886	7.65,–2.57,0.882	M	53	2	+/–	1	2.7	65
	1946	1921	7.94,–2.34,0.907	7.65,–2.57,0.882	M	16	5	+/–	1	2.7	65
	1949	2013	8.22,–2.03,0.962	8.18,–2.29,–0.008	M	13	4	+/–	1	3.6	160
	1952	2013	8.22,–2.03,0.958	8.18,–2.29,–0.008	M	6	3	+/–	1	3.6	160
	2005	2013	8.22,–2.04,0.943	8.18,–2.29,–0.008	M	21	3	+/–	1/2	3.6	160
	2036	2013	8.37,–1.83,0.963	8.18,–2.29,–0.008	M	31	2	+/–	1	3.6	160
	2116	2146	8.59,–1.40,1.01	8.68,–1.17,0.873	M	66	8	+/–	2/3	2.9	115
	2155	2146	8.69,–0.936,1.07	8.68,–1.17,0.873	M	26	5	+/–	1/4	2.9	115
	2209	2146	8.70,–0.764,1.10	8.68,–1.17,0.873	M	17	3	+/–	1/2	2.9	115
	2214	2146	8.70,–0.701,1.10	8.68,–1.17,0.873	M	14	3	+/–	2/3	2.9	115
	2236	2248	8.68,–0.460,1.13	8.68,–0.294,0.948	M	24	4	+/–	2/3	3.4	125
295	1903	1925	8.09,–2.30,1.06	8.26,–2.10,1.06	M	5	3	+/–	1/3	2.4	120
	1905	1925	8.09,–2.30,1.06	8.26,–2.10,1.06	M	7	2	+/–	1	2.4	120
	1907	1925	8.09,–2.30,1.05	8.26,–2.10,1.06	M	10	4	+/–	1	2.4	120
	1909	1925	8.14.–2.25,1.06	8.26,–2.10,1.06	M	5	4	+/–	1	2.2	120
	1917	1925	8.18,–2.20,1.06	8.26,–2.10,1.06	M	25	2	+/–	1	2.4	120
	1919	1925	8.22,–2.15,1.06	8.26,–2.10,1.06	M	15	3	+/–	1/8	2.4	120
	1922	1925	8.22,–2.15,1.06	8.26,–2.10,1.06	M	25	3	+/–	1/7	2.4	120
	1924	1925	8.26,–2.10,1.07	8.26,–2.10,1.06	M	5	1	+/–	1	2.4	120
	1931	1925	8.30,–2.05,1.07	8.26,–2.10,1.06	M	5	2	+/–	1	2.4	120
	1935	1925	8.33,–2.00,1.07	8.26,–2.10,1.06	M	5	4	+/–	1/2	2.4	120
	1939	1925	8.37,–1.95,1.08	8.26,–2.10,1.06	M	10	2	+/–	1	2.4	120
	1941	1925	8.37,–1.95,1.07	8.26,–2.10,1.06	M	7	3	+/–	1	2.4	120
	1945	1925	8.40,–1.90,1.08	8.26,–2.10,1.06	M	5	3	+/–	1	2.4	120
	1948	1925	8.42,–2.03,0.660	8.26,–2.10,1.06	M	10	3	+/–	1	2.4	120
	1952	1925	8.42,–1.84,1.08	8.26,–2.10,1.06	M	7	3	–/+	1/2	2.4	120
	2256	2248	8.30,0.313,1.26	7.77,0.980,1.26	M	9	2	+/–	1	2.8	175
	2300	2248	8.26,0.376,1.26	7.77,0.980,1.26	M	21	3	+/–	1	2.8	175
	2303	2248	8.22,0.437,1.26	7.77,0.980,1.26	M	8	2	+/–	1	2.8	175
	2314	2248	8.14,0.560,1.26	7.77,0.980,1.26	M	14	2	+/–	1/3	2.4	175

Table 1. (continued)

Day	Event Time, UT	Crossing Time, UT	Event Position in R_E (GSM)	Crossing Position in R_E (GSM)	Region	A, nT	τ, min	Polarity of B_N	α/B	B_m/B_s	θ, deg
				1984							
306	0433	0503	6.84,–3.72,1.55	7.31,–3.44,1.75	M	31	3	+/–	1	2.2	110
	0436	0503	6.91,–3.72,1.60	7.31,–3.44,1.75	M	15	5	+/–	1	2.2	110
	0441	0503	6.91,–3.71,1.61	7.31,–3.44,1.75	M	21	2	+/–	1	2.2	110
	0443	0503	6.91,–3.71,1.62	7.31,–3.44,1.75	M	9	2	+/–	1	2.2	110
	0456	0503	7.19,–3.54,1.70	7.31,–3.44,1.75	M	9	3	+/–	1	2.2	110
321	0626	0423	7.21,–4.78,0.847	5.70,–5.18,1.64	S	30	4	+/–	1/8	1.4	155
	0943	1003	7.74,–1.59,2.45	7.67,–1.38,2.37	M	16	3	+/–	1	2.6	180
	0956	1003	7.69,–1.45,2.40	7.67,–1.38,2.37	M	26	3	+/–	1	2.6	180
	1004	1003	7.64,–1.32,2.35	7.67,–1.38,2.37	M	29	4	+/–	1	2.6	180
	1008	1003	7.61,–1.24,2.32	7.67,–1.38,2.37	M	13	2	+/–	1	2.6	180
	1014	1003	7.58,–1.16,2.30	7.67,–1.38,2.37	M	9	2	+/–	1	2.6	180
	1016	1003	7.58,–1.16,2.30	7.67,–1.38,2.37	M	9	2	+/–	1	3.1	180
	1023	1003	7.51,–1.02,2.24	7.67,–1.38,2.37	M	29	5	+/–	1	3.1	180
	1033	1003	7.43,–0.882,2.19	7.67,–1.38,2.37	M	18	4	+/–	1/2	3.3	180
				1986							
025	0552	0618	6.87,–3.11,2.60	7.24,–2.74,2.84	M	6	2	+/–	1	1.9	100
	0556	0618	6.94,–3.05,2.64	7.24,–2.74,2.84	M	7	4	+/–	1	1.9	100
	0600	0618	7.00,–3.01,2.67	7.24,–2.74,2.84	M	6	3	+/–	1	1.9	100
	0603	0618	7.00,–2.96,2.71	7.24,–2.74,2.84	M	8	2	+/–	1	1.9	100
	0604	0618	7.06,–2.92,2.74	7.24,–2.74,2.84	M	7	2	+/–	1	1.9	100
	0606	0618	7.06,–2.91,2.75	7.24,–2.74,2.84	M	17	2	+/–	1	1.9	100
	0622	0618	7.24,–2.72,2.86	7.24,–2.74,2.84	S	30	3	+/–	1	1.9	100
	0637	0628	7.45,–2.50,2.96	7.35,–2.62,2.90	M	27	4	+/–	1	1.5	65
	0644	0628	7.50,–2.44,2.99	7.35,–2.62,2.90	M	16	7	+/–	1/3	1.5	65
	0843	0844	8.16,–0.859,3.25	8.16,–0.858,3.25	S	29	2	+/–	1	1.4	65
	0845	0844	8.16,–0.856,3.25	8.16,–0.858,3.25	M	16	2	+/–	1	1.4	65
	0847	0844	8.16,–0.637,3.30	8.16,–0.858,3.25	M	10	1	+/–	1	1.4	65
	0859	0844	8.18,–0.660,3.24	8.16,–0.858,3.25	S	29	4	+/–	1	1.2	65
	0903	0844	8.18,–0.580,3.22	8.16,–0.858,3.25	S	18	3	+/–	1	1.2	65
	0906	0844	8.18,–0.591,3.22	8.16,–0.858,3.25	S	16	1	+/–	1	1.2	65
	0936	0923	8.16,–0.204,3.16	8.17,–0.334,3.19	S	74	5	+/–	1	1.9	125
	0938	0923	8.15,–0.143,3.16	8.17,–0.334,3.19	S	49	1	+/–	1	1.9	125
	0944	0923	8.14,–0.078,3.14	8.17,–0.334,3.19	S	56	2	+/–	1	1.9	125
	0946	0923	8.14,–0.076,3.14	8.17,–0.334,3.19	S	56	2	+/–	1	1.9	125
	0949	0923	8.12,–0.277,3.12	8.17,–0.334,3.19	S	42	1	+/–	1	1.9	125

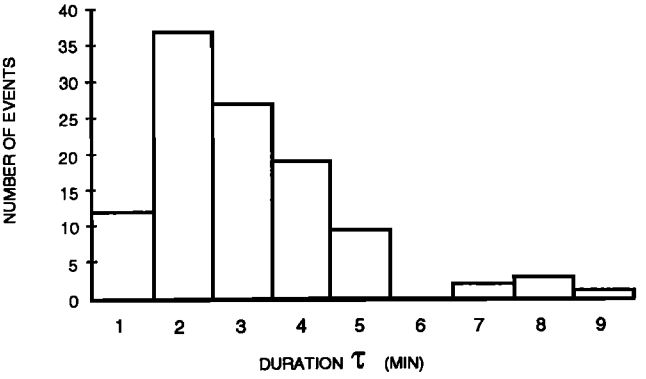

Figure 3. A histogram of event duration.

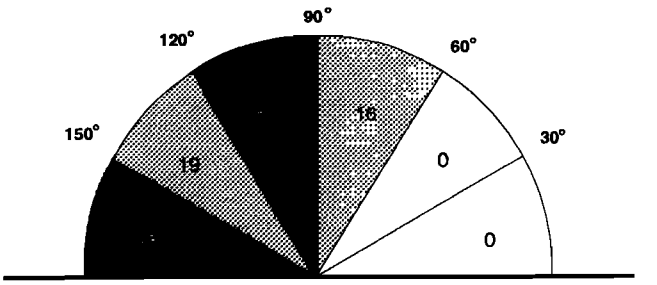

Figure 5. Distribution of events as a function of the angle between the magnetosheath and magnetospheric field components in the GSM y–z plane.

4.2. Duration and Amplitude

We consider the duration τ of an event to be the period during which there is a fluctuation in the magnetic field strength B from its ambient value. In nearly all cases, this fluctuation was an increase in the ambient field. In our data set, τ ranged from about 1 min to 9 min, with most events having short durations. The longest-duration events may have been the result of several shorter events that were merged. Figure 3 shows the distribution of event durations. The average duration of the events is about 3 min. As reviewed by *Sanny et al.* [1996], most researchers (including *Kawano and Russell* [1996]) have imposed a minimum duration of 30 s to 1 min when identifying events. By comparison, *Elphic* [1990] reported that FTEs typically exhibit durations much less than 1 min.

The amplitude A of an event is taken to the peak-to-peak value in the B_N signature. The distribution of amplitudes (see Figure 4) ranged from 5 nT to just above 150 nT, with an average of 47 nT for magnetosheath events and an average of 17 nT for magnetospheric events.

4.3. Magnetosheath Magnetic Field Orientation

Our events were observed near magnetopause crossings. Hence we were able to reliably obtain the relative orientation of the magnetic field vectors in the magnetosheath (which reflects that of the IMF) and the magnetosphere by comparing the field components on either side of each magnetopause crossing. As expected for FTEs, our events generally occurred for southward IMF. Figure 5 summarizes our results. It shows the distribution of the events as a function of the angle between the magnetosheath and magnetospheric field components in the GSM y–z plane. Of the 110 events, 94 occurred when this angle was greater than 90°; i.e., for a southward magnetosheath field. The remaining 16 events were observed for angles in the range between 60° and 90°, so the magnetosheath field had a weak northward component. There were no events observed for angles less than 60° or a strongly northward magnetosheath field. Examples of magnetopause crossings when the magnetosheath field was strongly northward can be found from 1700 to 1800 UT, day 305, 1984. We estimate that the angle between the magnetosheath and the magnetospheric field components in the GSM y–z plane was less than 10° at the time of these crossings. We were unable to discern any clear FTE signatures during that time interval.

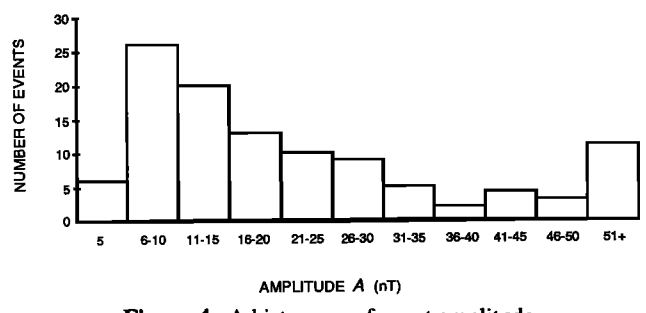

Figure 4. A histogram of event amplitude.

4.4. Magnetic Field Signature

The "classic" magnetic signature of an FTE is generally considered to be an increase in B, a symmetric bipolar fluctuation in B_N, and monopolar fluctuations in the other two components. We quantify the symmetry of the bipolar fluctuation using the ratio α/β, where α and β are the amplitudes of the leading and trailing pulses, respectively. The majority of our events (79 out of 110) exhibited symmetric or nearly symmetric signatures. As a general rule, we consider a signature to be symmetric or nearly symmetric if $\alpha \geq 0.75\beta$. The other 30 events were characterized by asymmetric B_N signatures in which the trailing pulse dominated; i.e., $\alpha/\beta < 0.75$. Figure 6 presents the variety in the magnetic signatures observed. The top three panels indicate the field components B_1, B_2, and B_3 along the directions of minimum, intermediate, and maximum variance, respectively, of the field. The bottom panel shows the total field B. The minimum-variance component B_1 is equivalent to B_N, the field component normal to the nominal magnetopause, and will be referred to as such. Figure 6a shows a prominent FTE in the magnetosheath centered on 1819 UT. This event is characterized by a symmetric bipolar fluctuation in B_N and an increase in B. Figure 6b also shows an FTE in the magnetosheath, centered on 0626 UT. This event has a highly asymmetric signature in B_N with a dominant trailing pulse. The asymmetric signature is accompanied by an increase in B. In Figure 6c we see a magnetospheric FTE centered on 1033 UT with an asymmetric B_N signature accompanied by a decrease in B, indicating that the spacecraft may have entered the event. Sometimes the orientation of the magnetopause may change noticeably between the time of a magnetopause crossing and when an event is observed. For example, Figure 6c presents an event in which the component of the magnetic field in the direction normal to the boundary is nonzero. The reason is that the magnetopause crossing used to determine the boundary normal occurred 30 min earlier (the limiting time criterion for this study). During that interval, the magnetopause orientation had changed. However, this does not preclude our ability to identify and use that event in our study. In a coordinate system that is rotated from the boundary normal system by an angle θ, the ratio α/β, our measure

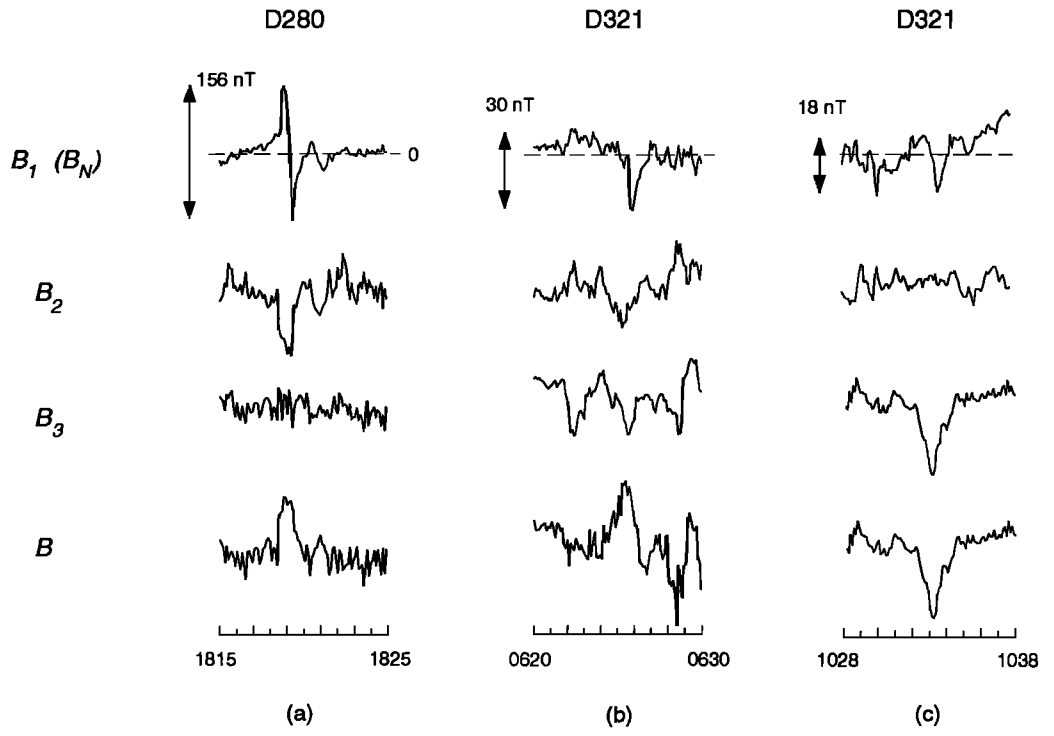

Figure 6. Various magnetic signatures observed in this study.

of symmetry in the bipolar signature, remains the same since both α and β are reduced by the factor cos θ.

Of the 26 events observed in the magnetosheath, 5 (or about 19%) were asymmetric and 21 were symmetric. Asymmetric events were observed more frequently in the magnetosphere, where of the 84 events in our data set, 26 (or about 31%) were asymmetric and 58 were symmetric. We found little difference between the average duration of the symmetric events and that of the asymmetric events. The average amplitudes of our symmetric and asymmetric events are also about the same at 24 and 25 nT, respectively.

Nearly all the asymmetric events occurred at low latitudes, as indicated in Figure 2. Most of these events seemed to occur in a band near $z_{GSM} = 1\ R_E$. Only 2 of the 30 asymmetric events were found poleward of $z_{GSM} = 1.5\ R_E$.

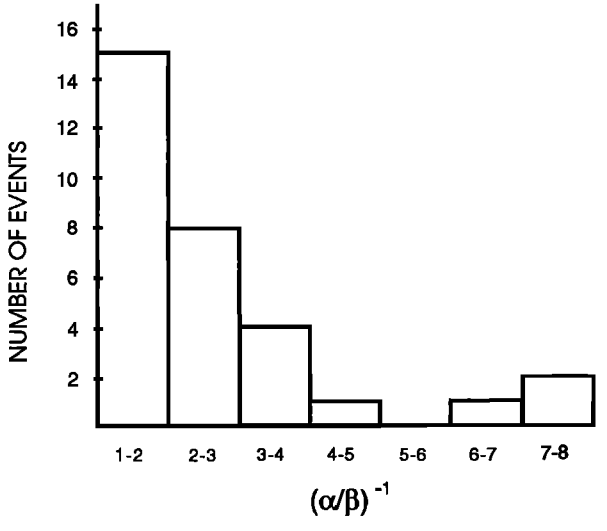

Figure 7. A histogram showing the relative degree of asymmetry in the asymmetric events of this study.

Figure 7 presents a histogram of asymmetry within our events. The majority of the events exhibit a low degree of asymmetry. For example, 23/31 or 74% of the events exhibit $(\alpha/\beta)^{-1} \leq 3$. The highest degree of asymmetry observed occurred in two cases when the trailing pulse of the B_N signature had an amplitude 7 to 8 times greater than that of the leading pulse.

4.5 Occurrence Versus B_m/B_s

As discussed earlier, the ratio of the field strengths in the magnetosphere and the magnetosheath B_m/B_s is an important factor determining the amplitudes of FTEs in two-dimensional MHD simulations. Generally, these simulations predict that both magnetosheath and magnetospheric FTEs can be observed if B_m/B_s is below a certain cutoff value, of the order of 1.5 to 2 for single X line models and 2.5 to 3 for multiple X line models. Above these respective cutoff values, magnetospheric FTEs are undetectable. We now consider the occurrence of our events as a function of B_m/B_s.

The 26 magnetosheath FTEs were all observed for low values of B_m/B_s. Of the 26 events, 23 (or nearly 90%) occurred for $B_m/B_s < 2$, while the other 3 occurred for $2 < B_m/B_s < 3$, as shown in Figure 8 (top panel). For these three events, B_m/B_s was only slightly above 2, at about 2.1 to 2.2.

FTEs were also observed with greater frequency in the magnetosphere for low values of B_m/B_s. However, in contrast to the magnetosheath events, only 26% (22 out of 84) were found to occur when $B_m/B_s < 2$ (see Figure 8, inverted panel). The highest number of events (40) was detected in the range $2 < B_m/B_s < 3$, with a sharp decrease in the occurrence rate above $B_m/B_s = 3$. These results appear to support the higher cutoff $B_m/B_s \approx 2.5$–3 for the multiple X line models as opposed to $B_m/B_s \approx 1.5$–2 for the single X line models. However, the detectability criterion used in obtaining these cutoff values is a peak-to-peak amplitude in B_N greater than or equal to 10 nT [*Ding et al.*, 1991]. We have used a detectability criterion of 5 nT for our magnetospheric FTEs. For this case, the

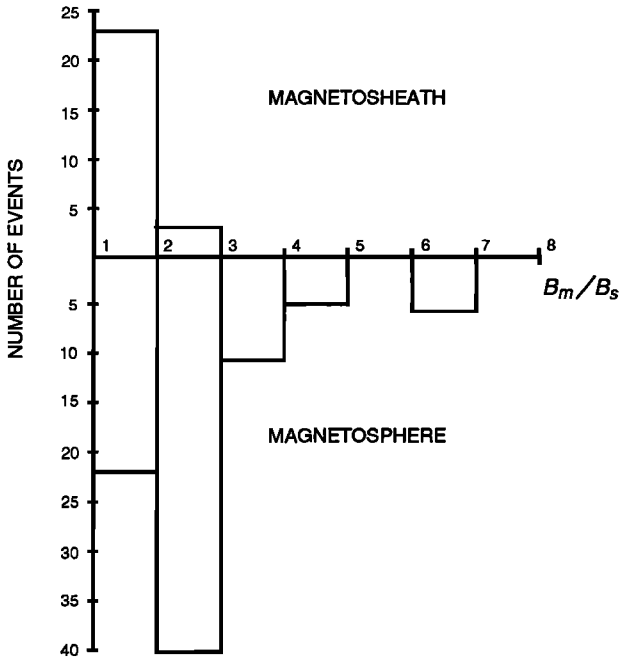

Figure 8. Occurrence of events in the magnetosheath and in the magnetosphere as a function of the ratio B_m/B_s.

cutoff in B_m/B_s is increased to about 2.5 to 3 for the single X line models and about 3.5 to 4 for the multiple X line models (for example, see *Ding et al.* [1991, Figure 5]). Hence we do not feel that the results shown in Figure 8 favor one model over the other.

Figure 9 is a plot of the average amplitude $\bar{A}$ of our magnetospheric FTEs as a function of B_m/B_s. There does not appear to be any strong dependence of $\bar{A}$ on B_m/B_s. However, as noted in the figure caption, there were far fewer events at higher values of B_m/B_s, so the statistical value of $\bar{A}$ is questionable above $B_m/B_s = 4$. Finally, symmetric events occurred more frequently within all the ranges of B_m/B_s shown.

5. Discussion

In our survey we found that FTEs with symmetric bipolar fluctuations in the magnetic field component normal to the nominal magnetopause had an occurrence rate between 2 and 3 times higher than that of FTEs with asymmetric fluctuations. Of the 110 events in our data set, 79 (or 72%) were symmetric and 31 (28%) were asymmetric. Although it is difficult to make a direct comparison with previous statistical studies, we believe that the relative occurrence of asymmetric events seen here is higher than in those studies. For example, without giving any quantitative comparison, *Rijnbeek et al.* [1984] state that "the vast number of FTEs observed are of the standard type, while only a relatively small number of irregular FTEs are observed." Perhaps the reason we observe a higher percentage of asymmetric events is that our data come from the CCE spacecraft rather than from the ISEE, which has hitherto been the principal source of information concerning magnetopause FTEs. The CCE has a nearly equatorial orbit with an apogee of 8.8 R_E. As a result, our data set consists of FTEs that (1) are generally at low latitudes and (2) occur when the magnetosphere has been severely compressed by the solar wind.

Although it seems much more likely that the onset of merging should occur along a single X line rather than simultaneously along multiple X lines, single X line simulations produce asymmetric FTEs (rarely observed), whereas multiple X line simulations produce symmetric FTEs (commonly observed). It is interesting to note from Figure 2 that most of the asymmetric events in our data set occur in the region near the magnetic equator. Only 2 of the 31 asymmetric events occur above $z_{GSM} = 1.5\ R_E$. This is consistent with simulation results which indicate that the signatures of FTEs produced by merging at a single X line evolve from an initial asymmetric form [*Ku and Sibeck*, 1997] into the familiar symmetric bipolar fluctuation commonly observed. Since the ISEE spacecraft detects a greater percentage of events at higher latitudes than the CCE, any statistical study based on ISEE data would be dominated by events with symmetric bipolar signatures.

Our premise of the evolution of the FTE bipolar signature may also explain the lower occurrence rate for asymmetric events in the magnetosheath (5 out of 26) than in the magnetosphere (26 out of 84). As noted earlier, the noise levels are greater in the magnetosheath than in the magnetosphere. Many smaller-amplitude events in the magnetosheath may have been masked by the noise, whereas similar events in the magnetosphere were not. A magnetosheath event recently formed, with an asymmetric B_N fluctuation, may have an amplitude that is below detectability thresholds. As a magnetosheath event moves away from the X line, its amplitude may increase sufficiently so that it becomes observable. However, at this point, its magnetic signature may have evolved into its symmetric form. As a result, our collection of magnetosheath FTEs is dominated by symmetric events.

Neither the single nor the multiple X line theories account for the occurrence of magnetospheric events for values of B_m/B_s at 4 and higher (see Figure 8). Perhaps this is an effect of the special condition that the magnetosphere was under severe compression by the solar wind pressure when the FTEs in our data set were observed.

6. Conclusion

MHD models based on merging at a single X line predict asymmetric bipolar FTE magnetic signatures in the direction normal to the nominal magnetopause. Models based on merging with similar rates at multiple X lines predict that this signature is symmetrically bipolar. Previous surveys of FTEs have not compared the relative occurrence rates of symmetric and asymmetric events, only noting that the symmetric events are the "vast majority." In this paper, we made this comparison by considering the magnetic signatures of 110 FTEs observed near the dayside magnetopause. These events were obtained from CCE data when the spacecraft was within 30

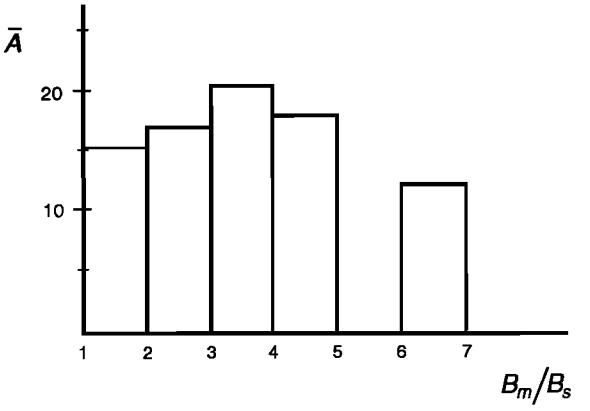

Figure 9. Average FTE amplitude in the magnetosphere as a function of B_m/B_s. The number of events observed for each interval is 22 for $1 < B_m/B_s < 2$, 40 for $2 < B_m/B_s < 3$, 11 for $3 < B_m/B_s < 4$, 5 for $4 < B_m/B_s < 5$, and 6 for $6 < B_m/B_s < 7$.

min of a magnetopause crossing. We found that a significant fraction of the events (31 out of 110) had B_N signatures that were not symmetrically bipolar. Most of the asymmetric events were observed in the magnetosphere. Furthermore, they appeared to occur generally near the magnetic equator.

Our results suggest that merging along a single X line may be an important source of FTEs. We suggested that the relatively high occurrence rate of asymmetric events near the magnetic equator is consistent with expectations for magnetic merging in this region, but that the asymmetric signature of an FTE evolves into the familiar symmetrically bipolar form as events travel to higher latitudes. Past statistical studies based on ISEE data would observe mostly symmetric events since the ISEE spacecraft detects a greater percentage of events at higher latitudes than the CCE.

Acknowledgments. We thank T. A. Potemra and the AMPTE CCE data center for supplying the CCE magnetometer observations. Work at LMU was supported by a Cottrell College Science Research Corporation Award and by the NASA/JOVE program. Work at APL was supported by NASA grant NAGW-3523.

The Editor thanks three referees for their assistance in evaluating this paper.

References

Berchem, J., and C. T. Russell, Flux transfer events on the magnetopause: Spatial distribution and controlling factors, *J. Geophys. Res., 89*, 6689, 1984.

Borodkova, N., G. Zastenker, and D. G. Sibeck, A case and statistical study of transient events at geosynchronous orbit and their solar wind origin, *J. Geophys. Res., 100*, 5643, 1995.

Ding, D. Q., L. C. Lee, and Z. F. Fu, Multiple X-line reconnection, 3, A particle simulation of flux transfer events, *J. Geophys. Res., 96*, 13,384, 1986.

Ding, D. Q., L. C. Lee, and Z. W. Ma, Different FTE signatures generated by the bursty single X-line reconnection and the multiple X-line reconnection at the dayside magnetopause, *J. Geophys. Res., 96*, 57, 1991.

Elphic, R. C., Observations of flux transfer events: Are FTEs flux ropes, islands, or surface waves?, in *Physics of Magnetic Flux Ropes, Geophys. Monogr. Ser.*, vol. 58, edited by C. T. Russell et al., 455 pp., AGU, Washington, D. C., 1990.

Farrugia, C. J., R. C. Elphic, D. J. Southwood, and S. W. H. Cowley, Field and flow perturbations outside the reconnected field line region in flux transfer events: Theory, *Planet. Space Sci., 35*, 227, 1987.

Gloeckler, G., et al., The Charge-Energy-Mass Spectrometer for 0.3–300 keV/e ions on the AMPTE CCE, *IEEE Trans. Geosci. Remote Sens., GE-23*, 234, 1985.

Haerendel, G., G. Paschmann, N. Sckopke, H. Rosenbauer, and P. C. Hedgecock, The frontside boundary layer of the magnetosphere and the problem of reconnection, *J. Geophys. Res., 83*, 3195, 1978.

Kawano, H., and C. T. Russell, Survey of flux transfer events observed with the ISEE 1 spacecraft: Rotational polarity and the source region, *J. Geophys. Res., 101*, 27,299, 1996.

Kawano, H., S. Kokubun, and K. Takahashi, Survey of transient magnetic field events in the dayside magnetosphere, *J. Geophys. Res., 97*, 10,677, 1992.

Ku, H. C., and D. G. Sibeck, Internal structure of flux transfer events produced by the onset of merging at a single X-line, *J. Geophys. Res., 102*, 2243, 1997.

Kuo, H., C. T. Russell, and G. Le, Statistical studies of flux transfer events, *J. Geophys. Res., 100*, 3513, 1995.

Lee, L. C., and Z. F. Fu, A theory of magnetic flux transfer at the earth's magnetopause, *Geophys. Res. Lett., 12*, 105, 1985.

Lee, L. C., and Z. F. Fu, Multiple X-line reconnection, 1, A criterion for the transition from a single X-line to a multiple X-line reconnection, *J. Geophys. Res., 91*, 6807, 1986.

Lin, Y., L. C. Lee, and M. Yan, Generation of dynamic pressure pulses downstream of the bow shock by variations in the interplanetary magnetic field orientation, *J. Geophys. Res., 101*, 479, 1996a.

Lin, Y., D. W. Swift, and L. C. Lee, Simulation of pressure pulses in the bow shock and magnetosheath driven by variations in interplanetary magnetic field direction, *J. Geophys. Res., 101*, 27251, 1996b.

Lockwood, M., S. W. H. Cowley, P. E. Sandholdt, and R. P. Lepping, The ionosphere signatures of flux transfer events and solar wind dynamic pressure changes, *J. Geophys. Res., 95*, 17,113, 1990.

Ma, Z. W., A. Otto, and L. C. Lee, Core magnetic field enhancement in single X-line, multiple X-line, and patchy reconnection, *J. Geophys. Res., 99*, 6129, 1994.

Potemra, T. A., L. J. Zanetti, and M. H. Acuña, The AMPTE CCE magnetic field experiment, *IEEE Trans. Geosci. Remote Sens., GE-23*, 246, 1985.

Rijnbeek, R. P., S. W. H. Cowley, D. J. Southwood, and C. T. Russell, A survey of dayside flux transfer events observed by ISEE 1 and 2 magnetometers, *J. Geophys. Res., 89*, 786, 1984.

Russell, C. T., and R. C. Elphic, Initial ISEE magnetometer results; Magnetopause observations, *Space Sci. Rev., 22*, 681, 1978.

Sanny, J., D. G. Sibeck, C. C. Venturini, and C. T. Russell, A statistical study of transient events in the outer dayside magnetosphere, *J. Geophys. Res., 101*, 4939, 1996.

Scholer, M., Magnetic flux transfer at the magnetopause based on single X-line bursty reconnection, *Geophys. Res. Lett., 15*, 291, 1988.

Shi, Y., C. C. Wu, and L. C. Lee, A study of multiple X-line reconnection at the dayside magnetopause, *Geophys. Res. Lett., 15*, 295, 1988.

Sibeck, D. G., and P. T. Newell, Pressure-pulse–driven surface waves at the magnetopause: A rebuttal, *J. Geophys. Res., 100*, 21,773, 1995.

Sibeck, D. G., and P. T. Newell, Reply, *J. Geophys. Res., 101*, 13,351, 1996.

Sibeck, D. G., et al., The magnetospheric response to 8-minute period strong-amplitude upstream pressure variations, *J. Geophys. Res., 94*, 2505, 1989.

Song, P., G. Le, and C. T. Russell, Observational differences between flux transfer events and surface waves at the magnetopause, *J. Geophys. Res., 99*, 2309, 1994.

Song, P., G. Le, and C. T. Russell, Comment on "Pressure-pulse–driven surface waves on the magnetopause: A rebuttal," by D. G. Sibeck and P. T. Newell, *J. Geophys. Res., 101*, 13,349, 1996.

Sonnerup, B. U. Ö., and L. J. Cahill Jr., Magnetopause structure and attitude from Explorer 12 observations, *J. Geophys. Res., 72*, 171, 1967.

Southwood, D. J., M. A. Saunders, M. W. Dunlop, W. A. C. Mier-Jedrzehowicz, and R. P. Rijnbeek, A survey of flux transfer events recorded by the UKS spacecraft magnetometer, *Planet. Space Sci., 34*, 1349, 1986.

Southwood, D. J., C. J. Farrugia, and M. A. Saunders, What are flux transfer events?, *Planet. Space Sci., 36*, 503, 1988.

Walthour, D. W., B. U. Ö. Sonnerup, G. Paschmann, H. Lühr, D. Klumpar, and T. Potemra, Remote sensing of two-dimensional magnetopause structures, *J. Geophys. Res., 98*, 1489, 1993.

Walthour, D. W., B. U. Ö. Sonnerup, R. C. Elphic, and C. T. Russell, Double vision: Remote sensing of a flux transfer event with ISEE 1 and 2, *J. Geophys. Res., 99*, 8555, 1994.

C. Beck and J. Sanny, Physics Department, Loyola Marymount University, Los Angeles, CA 90045. (e-mail: jsanny@lmumail.lmu.edu)

D. G. Sibeck, Applied Physics Laboratory, The Johns Hopkins University, Johns Hopkins Road, Laurel, MD 20723-6099. (e-mail: david.sibeck@jhuapl.edu)

(Received December 10, 1996; revised November 6, 1997; accepted November 6, 1997.)